Density and electric field fluctuations associated with the gradient drift instability in the high-latitude ionosphere

N. A. Gondarenko and P. N. Guzdar

Institute for Research in Electronics and Applied Physics, University of Maryland, College Park, Maryland, USA

Received 11 February 2004; revised 30 April 2004; accepted 10 May 2004; published 5 June 2004.

[1] The magnitudes of the density and electric field fluctuations and their spectral characteristics were studied with a three-dimensional nonlinear model of the structuring in high-latitude patches caused by the primary gradient drift instability. The simulations were compared with the simultaneous density and electric field spectra obtained from noon-midnight and dawn-dusk orbits of the Dynamic Explorer 2 (DE 2) satellite [*Basu et al.*, 1990]. The magnitudes of the simulated density and electric field fluctuations were found to be in very good agreement with the measured data. In the directions parallel and perpendicular to convection, the similarities in the spectral slope distributions of both simulated and observed density and electric field fluctuations were demonstrated. These findings together with our earlier results [*Gondarenko and Guzdar*, 1999, 2001, 2003; *Gondarenko et al.*, 2003] provide a significant evidence for coexistence of the primary gradient drift instability and subsequent secondary Kelvin-Helmholtz and tertiary shear-flow instabilities. *INDEX TERMS:* 2439 Ionosphere: Ionospheric irregularities; 2411 Ionosphere: Electric fields (2712); 7843 Space Plasma Physics: Numerical simulation studies. **Citation:** Gondarenko, N. A., and P. N. Guzdar (2004), Density and electric field fluctuations associated with the gradient drift instability in the high-latitude ionosphere, *Geophys. Res. Lett.*, *31*, L11802, doi:10.1029/2004GL019703.

1. Introduction

[2] Experimental studies of the high-latitude ionosphere indicate the presence of smaller-scale structures (tens of kilometers to 0.1 km scale sizes) on large-scale (hundreds of kilometers) enhanced plasma density regions identified as polar cap patches [*Weber et al.*, 1984, 1986; *Basu et al.*, 1988b, 1990; *Kivanç and Heelis*, 1997, 1998]. The observations of these interesting plasma structures have been reviewed by *Tsunoda* [1988], *Crowley* [1996], and *Basu and Valladares* [1999]. Spectral characteristics of smaller-scale irregularities at high latitudes have been studied using in situ measurements made by the DE 2 spacecraft [*Basu et al.*, 1988a, 1990; *Kivanç and Heelis*, 1997, 1998]. These studies provided a comprehensive description of the density and velocity small-scale irregularities of the patches. Using a quantitative patch definition introduced recently by *Coley and Heelis* [1995], *Kivanç and Heelis* [1997, 1998] investigated kilometer-size structures on patches convecting in the antisunward direction. They found a supportive evidence for the $E \times B$ drift instability operating in the polar cap region. Density spectral characteristics of the gradient drift instability (GDI) associated with polar cap ionization patches were reported by *Basu et al.* [1988b]. Later, *Basu et al.* [1990] provided a detailed description of the density and electric field spectra in two directions parallel and perpendicular to the antisunward convection. Although their high-resolution in situ data were considered in the orthogonal directions which were not sampled simultaneously, the provided statistical information on the density and electric field spectral indices could demonstrate the spectral behavior in these two directions. It has been concluded by the authors [*Basu et al.*, 1990] that it is important to consider the magnitudes of the density and electric field perturbations, as well as their spectral shape in order to determine the type of plasma instability responsible for the structuring.

[3] The investigation of the spectral characteristics of the irregularities and their magnitudes can contribute to identifying the mechanism of the mesoscale structuring in the high latitude ionosphere. Further, the experimental data can be compared with the results of numerical simulations describing a specific instability mechanism, and that can give indications on the source of the instability causing the electric field and density fluctuations at high latitudes. Among the various mechanisms, it is believed that interchangelike instabilities [*Keskinen and Ossakow*, 1982, 1983; *Keskinen and Huba*, 1990] are a major source of the ionospheric fluctuations of the intermediate scales (1–10 km). Numerical studies of the nonlinear evolution of the interchange $E \times B$ instabilities at high latitudes with scale-size-dependent magnetospheric coupling by *Keskinen and Huba* [1990] provided theoretical spectral indices for the density and electric field fluctuations in the directions parallel and perpendicular to the space craft trajectory, which were compared to the spectral slopes of the measured data by *Basu et al.* [1990]. Although these spectral characteristics were generally in agreement with the observations, the dynamics and evolution of the turbulent structures over the realistic time scale were not produced with the above model.

[4] In recent studies, *Guzdar et al.* [1998], *Gondarenko and Guzdar* [1999, 2001, 2003] have reported the results of the 3D nonlinear simulations, first for the collisional GDI, followed by the simulations with the ion inertial effects to model the mesoscale structures in plasma patches. For the purely collisional case, the basic structuring occurred transverse to the direction of the magnetic field and to the direction of the ambient density gradient in elongated "fingers". The inclusion of dynamics along the field line resulted in slowing down the structuring process [*Chaturvedi and Huba*, 1987]. It was found that anisotropy prevailed in power spectra of the electric field and density fluctuations in the plane transverse to the magnetic field

0094-8276/04/2004GL019703

[*Gondarenko and Guzdar*, 2001]. However, when ion-inertia processes associated with collisionless magnetospheric plasmas were considered, the spectra became more isotropic as was predicted in the simulation study by *Mitchell et al.* [1985]. *Gondarenko and Guzdar* [1999, 2001, 2003] have demonstrated that with the inclusion of the nonlinear ion inertial effects into the model, the secondary Kelvin-Helmholtz (KH) and tertiary shear-flow instabilities occur. The overall consequence of this hierarchy of instabilities is significant slowing down the structuring process that allows the patch to survive for many hours.

[5] Recently, *Gondarenko et al.* [2003] have demonstrated that the evolution of the structures is strongly influenced by the temporal variability of the flow since the GDI, which depends on the magnitude and direction of the flow velocity, is the primary instability that causes the structuring. If the flow velocity changes the direction of convection, structuring initially occurring on the trailing edge of the patch develops on the leading edge. In this study we show that the instability, in its full nonlinear development, penetrates through the patch and reaches the leading edge while the flow velocity remains a constant in time.

[6] The objective of this paper is to use the high-resolution data from our simulations to study the magnitude and spectral characteristics of the density and electric field structures with scale sizes ranging from about 40 km to 1 km. These data obtained with our parallel 3D finite-difference code have a dynamic range that allows us to make detailed comparisons with the observed spectral characteristics of the simultaneous density and electric field fluctuations derived from the DE 2 satellite data in two directions, parallel and perpendicular to the background plasma convection [*Basu et al.*, 1990].

2. Simulation Results

[7] The basic geometry for the high latitude plasma patch used in our three-dimensional (3D) nonlinear simulations is the following. The Earth's field lines are vertical and aligned with the z axis. The $-x$ axis points antisunward, and the y axis is orthogonal to the x and z directions. For these simulations we have considered the whole patch with the leading and trailing edges. The size of the box in the midnight-noon x and the dawn-dusk y directions are 400 km and 100 km, respectively. The size of the patch in the z direction is 1100 km. The density profile in x is a tanh function to model a localized patch and for the z dependence we use the Chapman function [*Guzdar et al.*, 1998; *Gondarenko and Guzdar*, 1999, 2001, 2003]. The peak density is assumed to be twice the background density at the height of $\sim$400 km (near the F peak height) [*Coley and Heelis*, 1995]. In our simulations we use the ion-neutral collision frequency profile [*Gondarenko and Guzdar*, 2003] with $\nu_{in} \sim 0.1\ \mathrm{s}^{-1}$ at the height of the density peak. The neutral wind velocity is $\vec{V}_n = V_n\vec{x}$. The electron continuity and vorticity equations [*Gondarenko and Guzdar*, 1999, 2001, 2003] are solved numerically, using our parallel 3D finite-difference code. The vorticity equation has contributions from the ion cross field current (Pedersen and polarization drifts) and the parallel resistive electron current. The electric field $\vec{E} = -\nabla\phi$, where ϕ is the electrostatic potential. The equilibrium potential is zero. We initialize the perturbed density/potential as a superposition of 70 sin/cos modes in the y direction with random phases and overall amplitude of 0.1%. The simulations were performed on a grid [1024, 1024, 52] with grid sizes Δx = 0.392 km, Δy = 0.098 km, and Δz = 22.4 km.

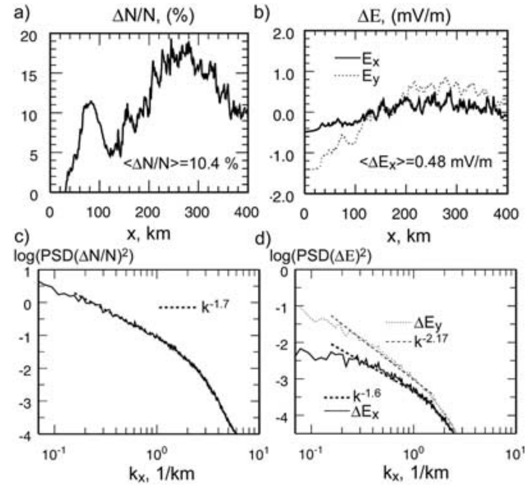

Figure 1. The amplitudes and power spectra of (a, c) $\Delta N/N$ and (b, d) ΔE in the x direction.

[8] In Figures 1a–1b we present the density $\Delta N/N$ (where $\Delta N = N - \langle N\rangle_y$) and electric field ΔE_x fluctuations computed from our nonlinear 3D simulations to be compared with the simultaneously obtained eight-second samples of the DE 2 satellite data along the midnight-noon direction of convection [*Basu et al.*, 1990, Figures 5 and 6]. The corresponding spectra of $\Delta N/N$ and ΔE_x obtained near the density peak in z and averaged over y are shown in Figures 1c–1d. The simulated density and electric field fluctuations are shown after about 1.8 hours when the structuring, initially occurred on the trailing (right) side of the patch, has penetrated almost through the entire patch. The magnitude of the averaged electric field fluctuations $\langle\sqrt{\langle\Delta E_x^2\rangle_y}\rangle_x$ is about 0.48 mVm^{-1} and the magnitude of the averaged density fluctuation $\langle\sqrt{\langle(\Delta N/N)^2\rangle_y}\rangle_x$ is about 10.44%. Using the detrending process, the density and electric field fluctuation spectral slopes were determined in the interval $k_x \in$ [0.16, 1.6] km^{-1} ($\sim$40–4 km in scale size). The spectral slope for the density fluctuations $\Delta N/N$ is 1.7 and for the electric field fluctuations ΔE_x and ΔE_y, the spectral indices are 1.6 and 2.17, respectively.

[9] Figures 2a–2d present the $\Delta N/N$ fluctuations with the corresponding ΔE_y (solid line) and ΔE_x (dotted line) fluctuations and their spectra to be compared with the simultaneously obtained density and electric field irregularity spectra for the dawn-dusk plane of the orbit orthogonal to the direction of convection [*Basu et al.*, 1990, Figures 13 and 14]. In this case, the spectral slopes were computed in the interval $k_y \in$ [0.6, 4.] km^{-1} ($\sim$10–1.6 km in scale size). Note that the density slope from the observations by *Basu et al.* [1990, Figure 13] was derived in the range from 8 km to 800 m in scale size.

[10] One interesting feature evident in the dawn-dusk direction spectra is that the electric field fluctuation spectrum is steeper than that in the midnight-noon direction. The spectral slopes for the simulated ΔE_y and ΔE_x are 2.4 and

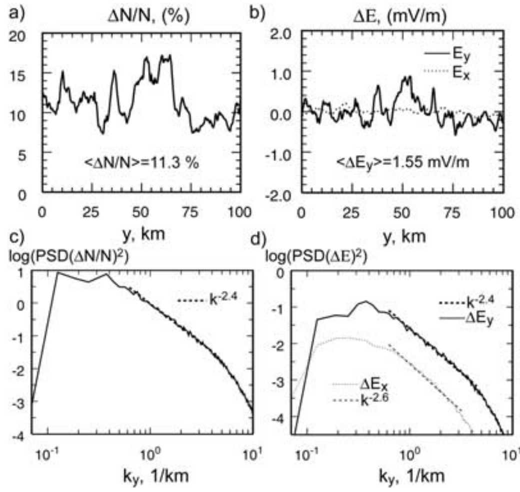

Figure 2. The amplitudes and power spectra of (a, c) $\Delta N/N$ and (b, d) ΔE in the y direction.

2.6, and the ΔE_y slope computed from the observations is 2.5. The simulated and observed ΔE_y spectral slopes are very close. The spectral slope for the simulated $\Delta N/N$ (Figure 2c) is 2.4 and it is steeper when compared with the spectral index 1.8 from the observations by *Basu et al.* [1990, Figure 13]. Note that in our case, ν_{in} (0.1 s^{-1}) at the F peak was significantly larger than the initial growth rate of the GDI (V_n/L_n = 0.01 s^{-1}). Since the shear flow and KH instabilities are both damped by the ion-neutral collisions, the dominant GDI produces the structures with different scale lengths in the x and y directions. Also, the long-wavelength parts of the simulated spectra may be influenced by the initial conditions for the density which is uniform in y and has a large gradient in the x direction. All these conditions could result in a discrepancy between the simulated $\Delta N/N$ slopes in the orthogonal directions that was not observed in the spectra by *Basu et al.* [1990, Figures 5 and 13].

[11] In Figures 3a–3c and Figures 3d–3f, we show histograms of the density and electric field fluctuation spectral slopes in the x and y directions, respectively. These distributions were obtained from the simulations of different patches with maximum densities two and three times the background density and at two late-time instances when the instabilities reached the leading edge. The spectral slopes in the direction of convection were obtained when the power spectra were averaged over each 10-km segment in the y direction while in the direction perpendicular to convection, the spectra were averaged over each 40-km segment in the x direction. We note that in the simulations with the increased density gradient, the density fluctuation amplitudes $\Delta N/N$ could be as large as ~22% that is of the same order as 15–20% reported by *Basu et al.* [1990].

[12] It has been found by *Basu et al.* [1990] that the spectral slopes of $\Delta N/N$ and ΔE_x in the direction of convection are identical. The measured density and electric field spectral slopes [*Basu et al.*, 1990, Figures 7a and 7b] have similar distributions with the peak value near 1.9 ± 0.1. However, these distributions are non-symmetric and similar to our case study, a tendency toward shallower slopes for the electric field is seen. In our case, within the error bounds (standard deviation of the mean), the mean values of the spectral indices for $\Delta N/N$, ΔE_x, and ΔE_y are 1.77 ± 0.03, 1.53 ± 0.03, and 2.21 ± 0.02, respectively.

[13] The simulated $\Delta N/N$ spectral indices of the k_y distribution vary from 1.8 to 3 with the mean value 2.27 ± 0.05, which is steeper than that in the x direction. In the distributions by *Basu et al.* [1990, Figures 15a and 7a], one can see a slight shift toward larger spectral slopes for the k_y distribution so that the mean value of the $\Delta N/N$ slopes in this direction is greater than that in the direction of convection. The steeper spectral indices of the density fluctuations in the direction perpendicular to convection were reported by *Keskinen and Huba* [1990]. They computed the spectral indices 1.8 ± 0.3 in the direction of convection and 2.2 ± 0.3 in the direction perpendicular to convection, using their model for the interchange $E \times B$ instability with scale-size-dependent magnetospheric coupling. However, in the direction of convection, the ΔE_x spectral slope (1.9 ± 0.3) computed by *Keskinen and Huba* [1990] is steeper than that (1.53 ± 0.03) from our model.

[14] Comparing the simulated (Figure 3e) and observed [*Basu et al.*, 1990, Figure 15b] spectral slope distributions, one can see that the widths of these distributions are very close. The simulated spectral slopes are ranging from 1.6 to 3.2 and the observed slopes from 1.4 to 3.4. The mean value of the simulated ΔE_y in the direction orthogonal to convection is about 2.33 ± 0.06 that is close to the mean value 2.24 ± 0.1 of the measured ΔE_y slopes [*Basu et al.*, 1990, Figure 15b] and to the spectral index 2.3 ± 0.3 computed for the interchange instability [*Keskinen and Huba*, 1990]. However, for the interchange instability, the ΔE_x slope (2.2 ± 0.3) in this direction is shallower than the corresponding ΔE_y slope and the mean value of the ΔE_x slopes (2.52 ± 0.07) computed from our simulations (Figure 3f).

[15] Another noticeable feature in these comparisons with the observations is that the magnitude of the electric field fluctuations ΔE_y in the y direction is larger than the ΔE_x magnitude in the x direction. *Basu et al.* [1990] derived the linear dependence between the ΔE magnitude

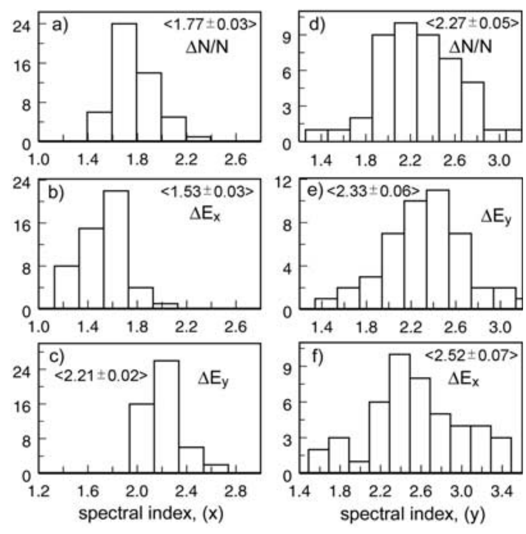

Figure 3. Histograms of spectral slopes of (a) $\Delta N/N$, (b) ΔE_x, and (c) ΔE_y in the x direction; (d) $\Delta N/N$, (e) ΔE_y, and (f) ΔE_x in the y direction.

(in millivolt per meter) and $\Delta N/N$ as follows: $\Delta E = 0.15(\Delta N/N)$. The maximum magnitude of the electric field ($\sim$1.55 mVm^{-1}) obtained from our simulations (Figure 2b) is in agreement with the value estimated with the above relation. $\Delta E/(\Delta N/N) = 1.55/11.34 = 0.137$. This ratio varies from 0.07 to 0.16 in our simulations.

[16] The distributions of the spectral indices in the x and y directions reveal an anisotropy of the density fluctuation spectra. This can be explained by the presence of the large initial density gradient in the x direction that results in the intrinsic difference between the x and y directions to start with. A similar anisotropy of the electric field fluctuation spectra is seen. This can be caused by the reduction of the shear flow generation because of the large value of the ion-neutral collision frequency at the density peak. The mechanism of the shear flow generation was discussed by *Gondarenko and Guzdar* [1999, 2001]. It was shown that with the smaller ion-neutral collisions, stronger shear flow was produced that resulted in a reduction of anisotropy in the spectra. Although the inertial effects could result in the production of more isotropic structures in the xy plane, a complete isotropization would not be possible because of the intrinsic asymmetry between the x direction of convection and the y direction of quasi-periodic variations of the structures.

[17] In conclusion, we have studied the magnitudes and spectral characteristics of the simulated density and electric field fluctuations obtained with our 3D model of the nonlinear evolution of the GDI, subsequent secondary KH, and tertiary shear-flow instabilities associated with structuring in high latitudes plasma patches. The high-resolution data from our simulations were compared with the observed simultaneous $\Delta N/N$ and ΔE fluctuations in the directions parallel and perpendicular to convection [*Basu et al.*, 1990]. The simulation results demonstrated the similarities with the observed spectral slope distributions of both density and electric field fluctuations in the direction of convection. In the direction perpendicular to convection, for the ΔE_y spectra, we found an increase in the range of spectral indices and steepening reported in the experiment. The difference in the measured ΔE_x and ΔE_y amplitudes in these two directions was also shown in the simulations. The magnitude of the electric field fluctuations was less than a few millivolts per meter. The amplitudes of the simulated $\Delta N/N$ and the relation between the ΔE and $\Delta N/N$ magnitudes were found to be in very good agreement with the measured characteristics reported by *Basu et al.* [1990].

[18] **Acknowledgments.** We acknowledge useful discussions with Dr. Sunanda Basu. This research was supported by the NSF under grant ATM-0122874 and in part by the NSF cooperative agreement ACI-9619020 through computing resources provided by the NPACI San Diego Supercomputer Center and Pittsburgh Supercomputer Center.

References

Basu, S., and C. Valladares (1999), Global aspects of plasma structures, *J. Atmos. Sol. Terr. Phys.*, *61*, 127.
Basu, S., S. Basu, E. MacKenzie et al. (1988a), Simultaneous density and electric field fluctuation spectra associated with velocity shears in the auroral oval, *J. Geophys. Res.*, *93*, 115.
Basu, S., S. Basu, E. J. Weber, and W. R. Coley (1988b), Case study of polar cap scintillation modeling using DE-2 irregularity measurements at 800 km, *Radio Sci.*, *23*, 545.
Basu, S., E. Mackenzie, W. R. Coley et al. (1990), Plasma structuring by the gradient-drift instability at high latitudes and comparison with velocity-shear driven processes, *J. Geophys. Res.*, *95*, 7799.
Chaturvedi, P. K., and J. D. Huba (1987), The interchange instability in high latitude plasma blobs, *J. Geophys. Res.*, *92*, 3357.
Coley, W. R., and R. A. Heelis (1995), Adaptive identification and characterization of polar ionization patches, *J. Geophys. Res.*, *100*, 23,819.
Crowley, G. (1996), Critical review on ionospheric patches and blobs, in *The Review of Radio Science*, p. 1, Oxford Univ. Press, New York.
Gondarenko, N. A., and P. N. Guzdar (1999), Gradient drift instability in high latitude plasma patches: Ion inertial effects, *Geophys. Res. Lett.*, *26*, 3345.
Gondarenko, N. A., and P. N. Guzdar (2001), Three-dimensional structuring characteristics of high-latitude plasma patches, *J. Geophys. Res.*, *106*, 24,611.
Gondarenko, N. A., and P. N. Guzdar (2003), Structure of turbulent irregularities in high-latitude plasma patches—3D nonlinear simulations, in *Disturbances in Geospace: The Storm-Substorm Relationship*, *Geophys. Monogr. Ser.*, vol. 142, edited by A. S. Sharma, Y. Kamide, and G. S. Lakhina, p. 205, AGU, Washington, D. C.
Gondarenko, N. A., P. N. Guzdar, J. J. Sojka, and M. David (2003), Structuring of high latitude plasma patches with variable drive, *Geophys. Res. Lett.*, *30*(4), 1165, doi:10.1029/2002GL016437.
Guzdar, P. N., N. A. Gondarenko, P. K. Chaturvedi, and S. Basu (1998), Three-dimensional nonlinear simulations of the gradient drift instability in the high-latitude ionosphere, *Radio Sci.*, *33*, 1901.
Keskinen, M. J., and J. D. Huba (1990), Nonlinear evolution of high-latitude ionospheric interchange instabilities with scale-size-dependent magnetospheric coupling, *J. Geophys. Res.*, *95*, 15,157.
Keskinen, M. J., and S. L. Ossakow (1982), Nonlinear evolution of convecting plasma enhancements in the auroral ionosphere: 1. Long wavelength irregularities, *J. Geophys. Res.*, *88*, 144.
Keskinen, M. J., and S. L. Ossakow (1983), Nonlinear evolution of convecting plasma enhancements in the auroral ionosphere: 2. Small-scale irregularities, *J. Geophys. Res.*, *87*, 474.
Kivanç, Ö., and R. A. Heelis (1997), Structures in ionospheric number density and velocity associated with polar cap ionization patches, *J. Geophys. Res.*, *102*, 307.
Kivanç, Ö., and R. A. Heelis (1998), Spatial distribution of ionospheric plasma and field structures in the high-latitude *F* region, *J. Geophys. Res.*, *103*, 6955.
Mitchell, H. G., J. A. Fedder, M. J. Keskinen, and S. T. Zalesak (1985), A simulation of high latitude F-layer instabilities in the presence of magnetosphere-ionosphere coupling, *Geophys. Res. Lett.*, *12*, 283.
Tsunoda, R. T. (1988), High-latitude F region irregularities: A review and synthesis, *Rev. Geophys.*, *26*, 719.
Weber, E. J., J. Buchau, J. G. Morre et al. (1984), F layer ionization patches in the polar cap, *J. Geophys. Res.*, *89*, 1683.
Weber, E. J., et al. (1986), Polar cap F patches: Structure and dynamics, *J. Geophys. Res.*, *91*, 12,121.

N. A. Gondarenko and P. N. Guzdar, Institute for Research in Electronics and Applied Physics, University of Maryland, College Park, MD 20742, USA. (ngondare@umd.edu; guzdar@glue.umd.edu)